J Appl Electrochem (2009) 39:329–337
DOI 10.1007/s10800-008-9676-2

ORIGINAL PAPER

Electrooxidation and inhibition of the antibacterial activity of oxytetracycline hydrochloride using a RuO_2 electrode

A. Rossi · V. A. Alves · L. A. Da Silva · M. A. Oliveira · D. O. S. Assis · F. A. Santos · R. R. S. De Miranda

Received: 13 February 2008 / Accepted: 29 September 2008 / Published online: 24 October 2008

Abstract This work reports on the electrochemical oxidation of oxytetracycline hydrochloride (OTCH) [(4S, 4aS,5aS,6S,12aS)-4-dimethylamino-1,4,4a,5, 5a,6,11,12a-octahydro-3,6,10,12,12a-hexahydroxy-6-methyl-1,11-dioxonaphthacene-2-carboxamide] on a RuO_2 electrode (DSA®) by cyclic voltammetry and electrolysis. The electrocatalytic efficiency of the electrode material was investigated as a function of different aqueous buffer solutions with pH values of 2.10 and 5.45 as supporting electrolytes. Spectrophotometric studies have shown that OTCH is stable in such solutions. The electrochemical degradation of OTCH is pseudo-first order at both pH values investigated with rate constants, k, of 9.9×10^{-5} s^{-1} (pH 2.10) and 1.9×10^{-4} s^{-1} (pH 5.45) at 21 ± 1 °C. Microbiological studies with *Staphylococcus aureus* ATCC 29213 have shown that OTCH lost antibacterial activity after 120 min of electrolysis at 50 mA cm^{-2}.

A. Rossi (✉) · V. A. Alves · M. A. Oliveira · D. O. S. Assis
Departamento de Farmácia, Faculdade de Ciências Biológicas e da Saúde, Universidade Federal dos Vales do Jequitinhonha e Mucuri/UFVJM, Rua da Glória 187, Centro. CEP: 39.100-000, Diamantina, Minas Gerais, Brazil
e-mail: alexandre.rossi@ufvjm.edu.br

L. A. Da Silva · R. R. S. De Miranda
Departamento de Química, Universidade Federal dos Vales do Jequitinhonha e Mucuri/UFVJM, Rua da Glória 187, Centro. CEP: 39. 100-000, Diamantina, Minas Gerais, Brazil

F. A. Santos
Departamento de Ciências Básicas, Universidade Federal dos Vales do Jequitinhonha e Mucuri/UFVJM, Rua da Glória 187, Centro. CEP: 39. 100-000, Diamantina, Minas Gerais, Brazil

Keywords Oxytetracycline · Oxide electrodes (DSA®) · Electrochemical oxidation · Electrochemical treatment of effluents

1 Introduction

In recent years, the contamination of soils and many waterways by drugs has attracted worldwide attention [1–6]. Within the spectrum of drugs, antibiotics deserve special attention due to the major environmental problems they cause, such as, (a) persistent molecular presence and microbiological impact (50–90% of dosages are excreted unaltered and persist in the environment) [7], (b) water contamination due to their widespread and indiscriminate use [2, 8], and (c) the great potential for the development of microbial resistance [9, 10]. In addition to the therapeutic and indiscriminate use of antibiotics to control bacterial infection in humans and animals, the pharmaceutical industry and hospital effluents are cited as being responsible for the increasing concentration of antibiotics in surface water from ng dm^{-3} to μg dm^{-3} [11, 12].

The contamination of bodies of water by antibiotics is aggravated by the limitations of conventional water treatment processes employed by effluent treatment stations (ETSs) responsible for supplying clean water to urban centres [13–15]. Thus, it is necessary either to implement treatment processes that increase the biodegradation or to remove antibiotics from water adequately by other means, complementing the processes already in place in the ETSs. Electrochemical processes have been studied extensively since 1980. It is a clean technology, as the main reactant is the electron. Electrochemical methods are also efficient in the treatment of organic pollutants [16–18]. This is an important technology these

days as human health and the environment are major concerns.

The efficient treatment of effluents depends mainly on the properties of an electrode material, such as mechanical and corrosion resistance, as well as physical-chemical stability at high anodic overpotential, which are indispensable requirements. Dimensionally stable anodes (DSA®), which combine high mechanical resistance with excellent electrocatalytic properties, are adequate candidates for the removal of organic pollutants [19, 20].

The analytical methods in the literature used to monitor the molecular degradation of antibiotics in watercourses are based mainly in liquid chromatography (HPLC), total organic carbon (TOC), spectrophotometry (UV–Vis), and mass spectrometry (MS) analysis [21–23]. However, these methods require skilled staff and costly, sophisticated equipment, which limit their application. In search of an alternative method, this work evaluates the molecular electrodegradation of oxytetracycline hydrochloride (OTCH) by means of a bacterial susceptibility test using *Staphylococcus aureus* ATCC 29213, which is based on its specific inhibition of bacterial protein synthesis. OTCH is mainly bacteriostatic, and *S. aureus* may act as a bacterial bioindicator of OTCH electrodegradation because it is sensitive to changes in the molecular structure of OTCH and the loss of antibacterial activity.

Studies on electrochemical degradation of antibiotics using DSA® and bacterial susceptibility test are almost inexistent in literature. Emphasis is given to the electrodegradation of aqueous effluents from industries, which contain phenols and primary alcohols, for applications in fuel cells [24, 25], utilizing chemical (DQO) and instrumental methods of analyses such as gas-chromatography-GC, High performance liquid chromatography-HPLC, mass spectrometry and others [24, 25].

In this work, a RuO_2 electrode (DSA®) was used in the electrooxidation and electrochemical degradation of OTCH in the presence of two different electrolytes buffered at pH 2.10 and 5.45, and used in a bacterial susceptibility test to evaluate the molecular electrodegradation of OTCH. The broad-spectrum antibiotic oxytetracycline hydrochloride was chosen in this work for its considerable use in Brazil, and for its solubility in water (0.5 g/cm^3 H_2O), which favours water contamination.

2 Experimental

2.1 Electrode preparation

Oxide layers of RuO_2 were deposited by thermal decomposition (T_{cal}: 400 °C) of a precursor solution, 0.1612 mol dm^{-3} $RuCl_3 \cdot nH_2O$ (Aldrich), in 1:1 (v/v) HCl:H_2O on both sides of sandblasted Ti supports (10 mm × 10 mm × 0.20 mm) previously etched for 20 min in boiling oxalic acid (10% w/w). The precursor solution was spread on both faces of the Ti-supports by brushing. The residue obtained after solvent evaporation at 80 °C was calcined for 10 min in preheated oven. The operation was repeated three to four times until the desired oxide loading, 2.3 mg cm^{-2} (nominal layer thickness ~2 μm), was obtained. Firing for 1 h in the same experimental conditions completed the procedure. The electrode preparation protocol was performed in duplicate. Details of the preparation and final mounting of the electrodes have been described elsewhere [26].

2.2 Solutions and antibiotic

The studies were carried out in two aqueous buffer solutions with an ionic strength (μ) of 0.80 mol dm^{-3} using citric acid/phosphate buffer [$HO_2CCH(CH_2CO_2H)_2$/Na_2HPO_4] and phosphate buffer [NaH_2PO_4/Na_2HPO_4] as supporting electrolytes, with pH values of 2.10 and 5.45, respectively. Distilled and purified water (Ionless® system, model 2500) was used as a solvent. OTCH, the study antibiotic was 99% pure (see Fig. 1). All reagents were of analytical grade and used without further purification.

2.3 Instrumentation and measurements

All electrochemical experiments were performed using a MicroQuímica®, model MQPG-01 potenciostat/galvanostat monitored by a computer. The cyclic voltammetry and bulk electrolysis experiments were performed in a 50 cm^3 one-compartment electrochemical cell with four openings adapted to receive the working electrode (RuO_2), the platinum spiral wire auxiliary electrode, the reference electrode (Ag/AgCl, sat.), and another port for solution sampling during electrolysis.

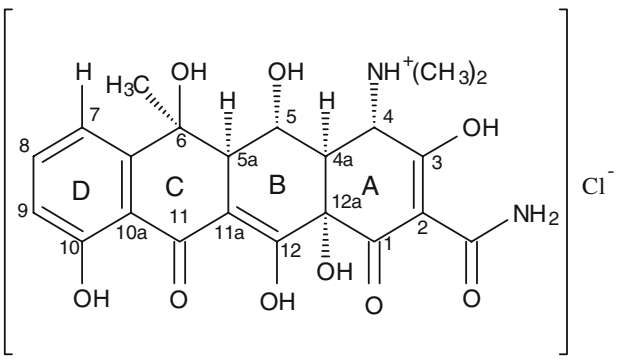

Fig. 1 Molecular structure of OTCH

Before each electrochemical experiment, freshly prepared RuO_2 electrodes were electrochemically activated by applying a constant anodic current with density of 50 mA cm^{-2} for 90 min using a chronopotenciometric program. The electrooxidation of 2.01×10^{-3} mol dm^{-3} OTCH was performed in either 35.00 cm^3 citric acid/phosphate buffer (pH 2.10) or phosphate buffer (pH 5.45) under magnetic agitation at constant anodic current density of 50 mA cm^{-2}.

Electrolyte samples of 1.00 cm^3 collected at different electrolysis times (0, 10, 20, 30, and 50 min) were diluted to 4.82×10^{-5} mol dm^{-3} and analysed by UV–Vis spectrophotometry to determine the kinetic parameters of the degradation. The spectra were recorded using a spectrophotometer from Micronal®, Model B-582 using quartz cells with 10 mm optical pathway.

The electrochemical degradation of OTCH after 120 min of electrolysis was investigated with a bacterial susceptibility test using *Staphylococcus aureus* ATCC 29213 inoculated at 37 °C in brain heart infusion (BHT) agar plates containing increasing concentrations of OTCH (2, 4, and 8 μg cm^{-3}) in samples collected during the electrolysis experiments. All the studies were carried out at room temperature (21 ± 1.0 °C).

3 Results and discussion

3.1 Electrode pre-treatment

To improve the reproducibility of the results during the electrooxidation of OTCH, which occurred simultaneously to the oxygen evolution reaction (OER), freshly prepared electrodes were pre-treated before each electrochemical experiment as described in the literature [27]. Freshly prepared coatings frequently show a significant increase in electrochemically active surface area after pre-treatment and reach equilibrium under intense OER [27]. In this work, the electrochemically active surface area of the RuO_2 electrode increased after treatment with either citric acid/Na_2HPO_4 buffer (pH 2.10) or phosphate buffer (pH 5.45) as supporting electrolytes, both with $\mu = 0.80$ mol dm^{-3}.

Electrode activation under intense OER is attributed to the hydration of surface sites in difficult-to-reach oxide regions (pores, small cracks, etc.) [27]. Pre-treatment must be performed to avoid changes in the electrochemically active surface area of the electrode during the electrochemical experiments. It was also used as a cleaning/regeneration method for the electrochemically active surface area of the RuO_2 electrodes after recording each cyclic voltammogram in the presence of OTCH, as apparently the electrodes are blocked by adsorbed organic films (dimers/polymers).

3.2 OTCH Stability by Spectrophotometry

The UV–Vis absorption spectra of OTCH in the presence of both supporting electrolytes (with different pH values (2.10 and 5.45) showed two characteristic bands with maximum absorption at 280 and 354 nm. These results are in accordance with literature [28]. The maximum absorption (A_{max}) values and the molar absorptivity coefficients (ε) at both pH values are shown in Table 1.

The A_{max} of OTCH at 280 nm is related to the chromophore part of the molecule, represented by an A in the ring [28, 29]. The β-hydroxyketo system at C10, C10a, C11, C11a, and C12 is the chromophore part BCD of OTCH, and is responsible for the absorption at 354 nm [29]. The molar absorptivity coefficients of OTCH shows a hyperchromic effect with increasing pH for both values of λ_{max}. This suggests that an increase in pH facilitates the electronic transitions $\pi \rightarrow \pi^*$ and $n \rightarrow \pi^*$ of the OTCH molecule.

The stability of OTCH was investigated through spectrophotometry to determine if any change in molecular structure is associated with its own decomposition or chemical reaction with the different supporting electrolytes (pH 2.10 and 5.45). Absorbance was measured in freshly prepared solutions for 24 h at 280 and 354 nm. In this time interval, the absorbance values remained constant as a function of time at both wavelengths and pH values. Thus, the molecular structure of OTCH remained unaltered in the presence of the supporting electrolytes.

The electrochemical study of OTCH in the presence of buffered supporting electrolytes was necessary because the active surface sites of the RuO_2 electrode are pH-dependent [30, 31]. The redox properties of the RuO_2 electrode may also be influenced by the acidic nature of the OTCH molecule and the acidification of the solutions during electrooxidation.

A previous study showed that the pH of a 2.01×10^{-3} mol dm^{-3} OTCH solution in the presence of KNO_3 decreased from 5.40 to 2.75 after the addition and dissolution of OTCH due to its acidity in aqueous solutions. The pH of that OTCH non-buffered solution submitted to electrolysis at constant current (50 mA cm^{-2})

Table 1 Wavelength values of maximum absorption (A_{max}) and the molar absorptivity coefficients (ε) of OTCH at different pH values

pH	[OTCH]/ mol dm^{-3}	Wavelength/ nm	A_{max}	ε/(mol dm^{-3})$^{-1}$ cm^{-1}
2.10	4.83×10^{-5}	280	0.783	16211
		354	0.618	12795
5.45	8.85×10^{-5}	280	1.824	20610
		354	1.537	17378

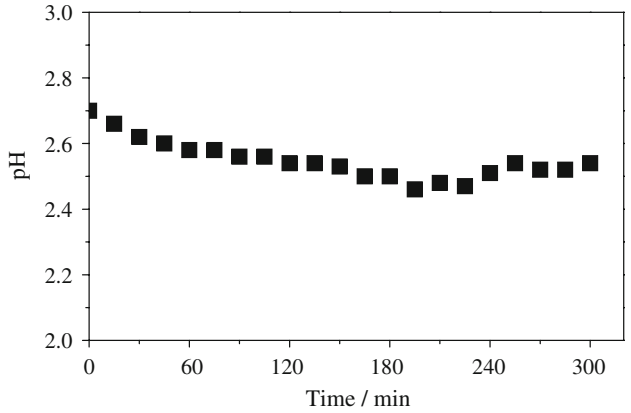

Fig. 2 Variation of pH during the electrochemical degradation of 2.01×10^{-3} mol dm^{-3} OTCH in 0.10 mol dm^{-3} KNO_3 using a RuO_2 electrode (geometric area of 2 cm^2)

for 5 h on the working RuO_2 electrode decreased by 0.3 pH units at most, as seen in Fig. 2. The decrease in the solution pH may be due to the oxidation/degradation of OTCH and the formation of aliphatic acids, which has also been proposed by other authors [32, 33]. However, the analysis of OTCH samples after electrooxidation for 30, 60, and 120 min by thin-layer chromatography on a silica stationary phase showed that the samples did not elute in either methanol or methanol:water (7:3, v:v), suggesting the formation of high polarity species such as aliphatic acids.

The pH values in non-buffered OTCH solutions at the end of 5 h electrolysis varied by almost 3 pH units. Obviously, higher variations of pH values may be obtained with longer electrolysis times, depending on the chemical nature of the antibiotic. However, a decrease of 1 pH unit is enough to change the electrocatalytic properties of oxide electrodes as a result of an anodic potential shift of almost 90 mV. This potential variation as a function of pH, which is related to the electrode electrocatalytic properties, was obtained by Burke and Whelan [31] through the relation $\Delta E = (1.5 \times 2.3RT/F) \times pH$, where the factor of 1.5 is the stoichiometric relation between H^+/e^- from reaction (1).

$$2\left[RuO_2(OH)_2 2H_2O\right]^{2-} + 2e^- + 3H^+ \rightarrow \left[Ru_2O_3(OH)_3 3H_2O\right]^{3-} + 3H_2O \quad (1)$$

In fact, when electrolysis of OTCH was carried out in a buffered solution, the pH did not vary. According to Cao et al. [34], systematic studies of the effect of solution pH on the electrocatalytic behavior of oxide electrodes during electrooxidation of organic compounds are needed. We observed that the changes in pH values, which resulted from the dissolution of OTCH in the supporting electrolyte and/or the formation of organic acids as molecular electrodegradation products of OTCH, might significantly alter the electrocatalytic properties of the degradation of OTCH when the electrode material is pH-dependent, as is RuO_2.

3.3 Cyclic voltammetry

The cyclic voltammograms of RuO_2 electrodes in supporting electrolytes of distinct chemical composition and pH values (2.10 and 5.45), in both the absence and the presence of 2.01×10^{-3} mol dm^{-3} OTCH, are shown in Fig. 3. In the absence of OCTH, the cyclic voltammograms show a broad peak corresponding to the Ru(IV)/Ru(III) (region I) and Ru(VI)/Ru(IV) (region II) redox transitions. The half-wave potential ($E_{1/2}$) values of the redox transitions shift to less positive potentials as the pH increases, as shown in Fig. 4. Additionally, the onset of the oxygen evolution reaction (OER) (region III), characterized by a rapid increase in current, is anticipated. Although these findings are corroborated by the literature, they were not obtained in buffered solutions [31]. In general, the behavior of DSAs® in buffered solutions do not differ significantly from those in $HClO_4$ [35] and H_2SO_4 [36], except for a shift of the redox transitions to less positive potentials as the pH increases.

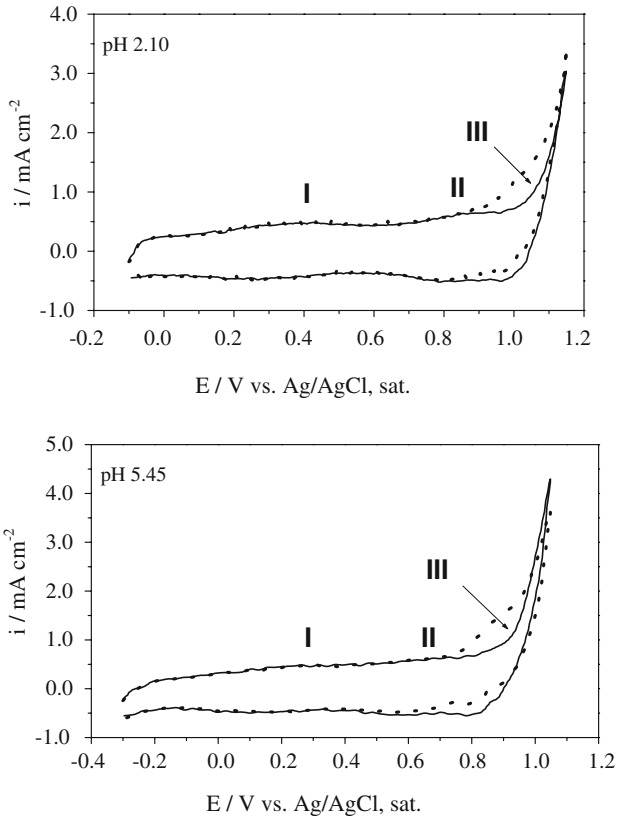

Fig. 3 Cyclic voltammograms of the RuO_2 electrode in the absence (—) and presence (…) of a 2.01×10^{-3} mol dm^{-3} OTCH solution, $v = 20$ mV s^{-1}

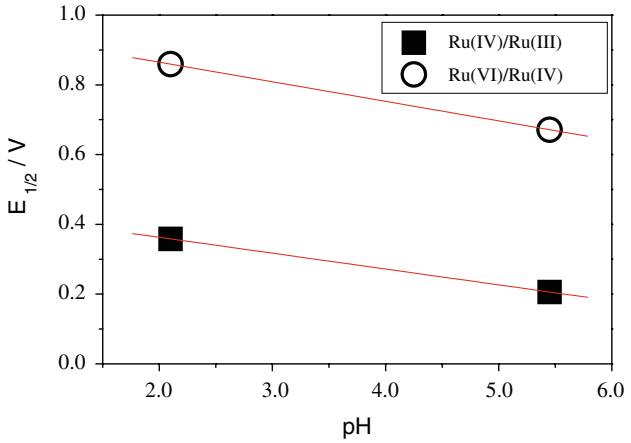

Fig. 4 Half-wave potential ($E_{1/2}$) variation of the redox transitions Ru(III/IV) and Ru(IV/VII) occurring at the RuO_2 electrodes as a function of pH

The cyclic voltammograms of 2.49×10^{-3} mol dm^{-3} OTCH solutions recorded at 40, 60, 80, 100, and 120 mV s^{-1} showed catalytic currents due to the antibiotic electrooxidation near the OER at approximately +0.90 V and +0.76 V verses Ag/AgCl, sat. at pH 2.10 and 5.45, respectively. At both pH values, the electrooxidation of OTCH seemed to be catalysed by the Ru(VI) species. At more positive potentials, at which OER occurs, a Ru(VII) species is probably responsible for the electrooxidation of OTCH. At both pH values, OTCH showed non-faradaic behavior in the potential intervals from −0.10 to +0.80 V (pH 2.10) and −0.30 to +0.70 V (pH 5.45) without electrode surface blockage. OTCH electrooxidizes by diffusion, as confirmed by the linear relationship between the oxidation current of OTCH (i_{ox}), measured at +0.88 V and pH 5.45 as a function of the scan rate square root ($v^{1/2}$), as shown in Fig. 5 [37]. This behavior was also observed at pH 2.10.

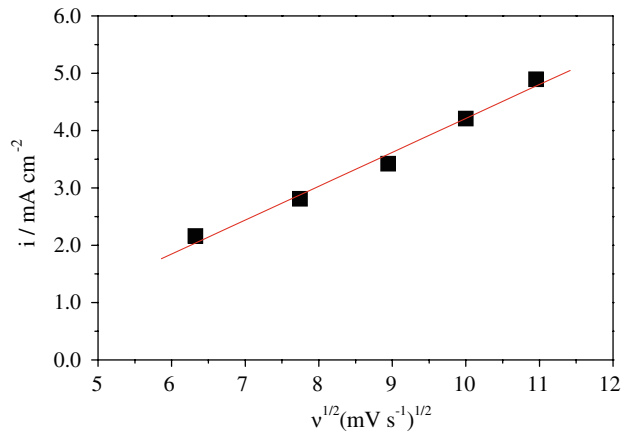

Fig. 5 Variation of the scan rate square root as a function of the catalytic current of electrooxidation of 2.49×10^{-3} mol dm^{-3} OTCH at pH 5.45

The electrooxidation of OTCH on a RuO_2 electrode with small current increases near the OER region has been reported for various organic compounds [38, 39]. High electrooxidation currents are observed for noble metal anodes, such as Pt and Au. Mousty et al. proposed that the transference of electrons for the oxidation of organic compounds requires low overpotentials and is associated with metallic sites present in the anodes [40]. The low metal content of the oxide electrodes may explain their low capacity for oxidizing organic compounds and the need for high overpotentials.

During the electrocatalytic oxidation of OTCH, the surface of the metal oxide electrode (RuO_2) suffers a water discharge and forms hydroxyl radicals, which are physically adsorbed on the electrode [41, 42], according to reaction (2):

$$RuO_x + H_2O \rightarrow RuO_x(OH^*) + H^+ + e^- \quad (2)$$

After reaction (2), the next step is the formation of an oxide in a higher oxidation state, which promotes the gradual oxidation of OTCH, as shown by reaction (4). In parallel to the gradual oxidation of OTCH, the higher oxidation state oxide species (RuO_{x+1}) may lead to the oxygen evolution reaction, according to reaction (5), which, in turn, may act in the oxidation/degradation of the OTCH molecule.

$$RuO_x(OH^*) \rightarrow RuO_{x+1} + H^+ + e^- \quad (3)$$

$$RuO_{x+1} + R_{OTCH} \rightarrow RuO_x + RO_{OTCH} \quad (4)$$

$$RuO_{x+1} \rightarrow RuO_x + {}^1/_2O_2 \quad (5)$$

According to Foti et al. [43], combustion of OTCH may occur, although it is less favoured than the gradual oxidation by the RuO_2 electrode. In the presence of organic compounds that may be oxidized, such as OTCH, the higher oxide RuO_{x+1} may lead to the formation of specific oxidation products (reaction 4). However, further reactions of the formed product with the higher oxide lead to the formation of aliphatic acids and then to CO_2, as shown by reactions (6) and (7). Alternatively, the hydroxyl radicals physically adsorbed on the metal oxide electrode may directly oxidize the OTCH molecule, as seen in reaction (8):

$$RuO_{x+1} + RO_{OTCH} \rightarrow ROOH \text{ (aliphatic acids)} \quad (6)$$

$$RuO_{x+1} + ROOH \text{ (aliphatic acids)} \rightarrow CO_2 + RuO_x \quad (7)$$

$$RuO_x(^\bullet OH) + R \rightarrow RuO_x + mCO_2 + nH_2O + H^+ + e^- \quad (8)$$

One of the problems in the use of metal oxide electrodes in the electrooxidation of organic compounds is the blockage of active surface sites [27, 36]. Consecutive cyclic voltammograms in the presence of 2.01×10^{-3} mol dm^{-3} OTCH showed active site blockage for both electrolyte solutions, pH 2.10 and 5.45.

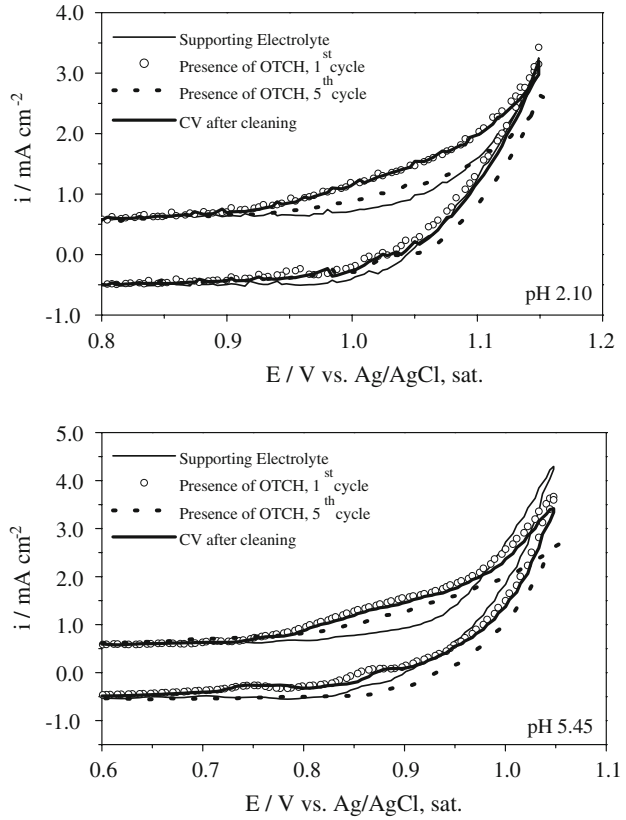

Fig. 6 Cyclic voltammograms of the RuO_2 electrode in presence of 2.01×10^{-3} mol dm^{-3} OTCH in buffered solution, $v = 20$ mV s^{-1}

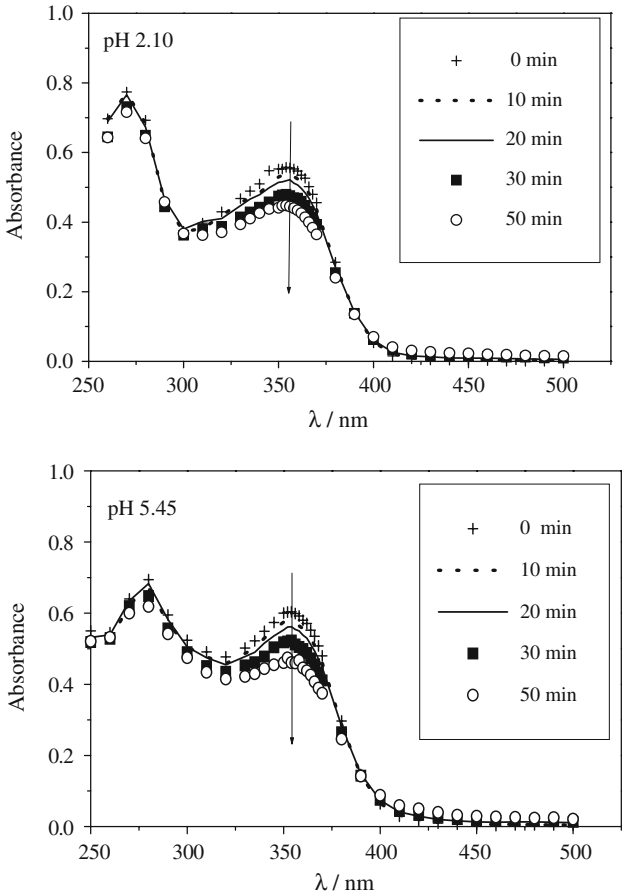

Fig. 7 Absorption spectra of buffered supporting electrolytes containing 4.82×10^{-5} mol dm^{-3} OTCH after different electrolysis times

Figure 6 supports the presence of this blockage of the RuO_2 active surface sites by a considerable decrease in the oxidation anodic current of OTCH. This behaviour suggests the adsorption of organic films formed by dimers/polymers or intermediate products from the molecular electrooxidation of OTCH, which obstructs the active surface sites on the oxide electrodes. However, pre-treatment of the RuO_2 electrodes allows the active surface sites to be regenerated, not only through the mechanical action and oxidizing power of OER, but also by the oxidation/degradation of the adsorbed film by the higher oxides and/or by the hydroxyl radicals formed on the electrode surface.

3.4 Kinetic studies of OTCH electrooxidation

The electrooxidation of 2.01×10^{-3} mol dm^{-3} buffered OTCH solutions (pH 2.10 and 5.45) was performed at a constant anodic current of +100 mA applied on the RuO_2 electrode. Samples of 1.00 cm^3 were collected at specific times during the OTCH electrolysis: 0, 10, 20, 30, and 50 min. UV–Vis spectra of diluted samples (4.82×10^{-5} mol dm^{-3}) were recorded immediately after sampling from 240 to 500 nm, Fig. 7.

These spectra show a decrease in absorbance at 280 and 354 nm as a function of electrolysis time. However, higher variations were observed at 354 nm (from 20 to 50 min). At this wavelength, this behavior is more pronounced at pH 5.45, which suggests that the molecular structure of OTCH was changed, such as by the degradation of the chromophore parts D, C, and B of the OTCH molecule (Fig. 1) mainly in the β-hydroxyketo system at C10, C10a, C11, C11a, and C12, which is responsible for the absorption at 354 nm [28, 29]. Considering A_{max} at 345 nm, the plot of ln (A/A_0) versus electrolysis time shows a linear relationship (Fig. 8), suggestive of the electrochemical degradation of OTCH in the presence of buffered supporting electrolytes (pH 2.10 and 5.45) by a pseudo-first order kinetics analysis of the OTCH concentration. Rate constants (k) of 9.9×10^{-5} s^{-1} ($r^2 = 0.9979$) and $1.9 \times {}^{-4}$ s^{-1} ($r^2 = 0.9933$) for pH values of 2.10 and 5.45, respectively, were obtained. The value of k, the rate of electrochemical degradation of OTCH on the RuO_2 electrode, was almost twice as large at pH 5.45 as at pH 2.10. According to Whelan and Burk [31], this result may be explained by the fact that the

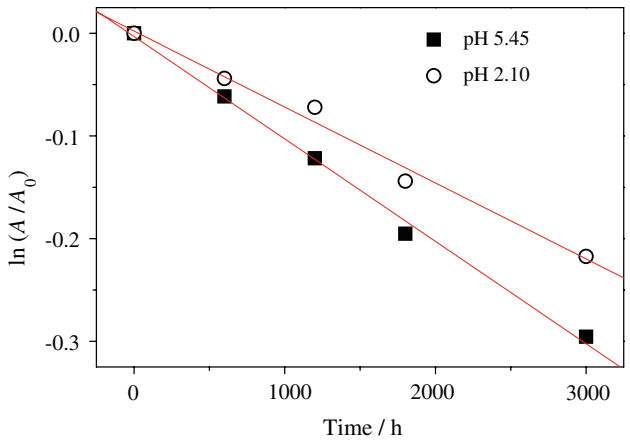

Fig. 8 Behavior of ln (A/A_0) of 4.82×10^{-5} mol dm^{-3} OTCH as a function of electrolysis time, $\lambda = 354$ nm

redox transitions occur at less positive potentials and that the overpotential is the lowest for the OER at the higher pH. Therefore, the variation of pH may influence the electrocatalytic potentialities of metal oxide materials regarding the electrochemical degradation of organic compounds, suggesting that it is favoured at pH 5.45.

3.5 Inhibition of antibacterial activity of OTCH

According to the k values obtained in the kinetics studies, the electrooxidation of a 2.01×10^{-3} mol dm^{-3} OTCH solution was carried out using the RuO_2 electrode applying a constant anodic current of 50 mA cm^{-2} for 120 min at pH 5.45. Samples of 1.00 cm^3 were collected from the OTCH solution before the electrolysis and after 30, 60, 90, and 120 min of electrolysis for microbiological and spectrophotometric analysis. The absorption spectra are shown in Fig. 9.

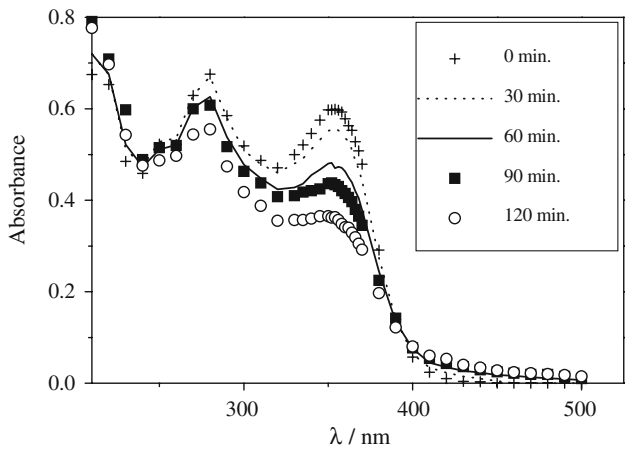

Fig. 9 UV–Vis spectra after electrodegradation of 4.82×10^{-5} mol dm^{-3} OTCH in phosphate buffer solution at pH 5.45, at different electrolysis times

Table 2 Bacterial susceptibility test of *Staphylococcus aureus* ATCC 29213 to OTCH in buffered phosphate solution at pH 5.45 treated by electrolysis for 120 min

MIC[a]/μg cm^{-3}	Time/min				
	0	30	60	90	120
2.0	+	+	+	+	+
4.0	−	+	+	+	+
8.0	−	−	−	−	+

[a] Minimum inhibitory concentration; +, presence of bacteria growth; −, absence of bacteria growth

In addition to the decrease in A_{max} values discussed previously, the samples collected during the electrooxidation of OCTH also showed a noticeable colour variation. The OTCH solution became darker after the first 30 min of electrooxidation, going from yellow-green to light brown. The colour changed gradually with the increase in the electrolysis time, until the solution turned dark brown, demonstrating the chemical transformation or the modification of the molecular structure of the organic compounds.

The molecular degradation of OTCH at different electrolysis times (0, 30, 60, 90, and 120 min) and the loss of its antibacterial activity were studied by microbiological analysis. The antibacterial activity of the samples collected during electrooxidation with different OTCH concentrations (2, 4, and 8 μg cm^{-3}) was tested with *Staphylococcus aureus* ATCC 29213 as a bioindicator. The minimum inhibitory concentrations (MIC) of the OTCH solutions are shown in Table 2.

The bacterial susceptibility results for *Staphylococcus aureus* ATCC 29213 to OTCH show that the value of MIC before the electrooxidation of the solution was 4.0 μg cm^{-3}. MIC indicates the minimum concentration of an antibiotic that completely inhibits the growth of *S. aureus* populations. After 30, 60, and 90 min of electrolysis of a 2.01×10^{-3} mol dm^{-3} OTCH solution, the MIC increased from 4.0 to 8.0 μg cm^{-3}. This increase suggests a partial loss of the OTCH′s antibacterial activity up to 90 min of electrolysis. Since some OTCH molecules suffered structural modification and lost their antibacterial activity, a higher concentration of OTCH (8.0 μg mL^{-1}) was necessary to inhibit the growth of *S. aureus*. However, 120 min of electrolysis resulted in the complete loss of the antibacterial activity. The products of electrooxidation and the rate of complete mineralization of the OTCH along with its partial or complete conversion to CO_2 and H_2O will be evaluated in future work. Even if OTCH mineralizes completely, the loss of its antibacterial activity as a function of a small modification of its molecular structure would minimize water pollution and the associated health hazards.

The stability of the RuO_2 electrode during the electrooxidation of OTCH at pH value 5.45 was monitored

through total voltammetric charge (Qt). The Qt values were obtained by the integration of the potential between −0.25 V and +0.88 V of the cyclic voltammograms recorded before and after electrolysis. The total voltammetric charges (Qt) of the RuO_2 electrode obtained before and after OTCH electrooxidation were 67.5 and 81.2 mC cm^{-2}, respectively. Instead of a decrease in the value of the voltammetric charge of the RuO_2 electrode, a normal occurrence for oxide electrodes submitted to prolonged intense oxygen evolution reaction (OER) [44], is the observed increase in Qt, which indicates the high stability of the RuO_2 electrode under the investigated experimental conditions of electrooxidation of OTCH. Although it suggests the electrode stability, this may also be related to the hydration of sites, pores, and/or microcracks not hydrated in the electrode pre-treatment.

One methodological aspect of this work that needs special attention is electricity consumption. In the experimental conditions of electrodegradation of OTCH, when a current of +0.1 A was applied to the RuO_2 anode, the cell potential was −10.7 V throughout the electrolysis. Considering the total time of 120 min, the time required for the total loss of the antibacterial activity of OTCH, the estimated electricity consumption necessary to inhibit the antibacterial activity of OTCH was 155 Wh g^{-1}.

4 Conclusions

RuO_2 electrodes efficiently electrooxidized OCTH in aqueous solution, making this technology a promising and complementary method to minimize the impact of antibiotics on aquatic ecosystems by its use at water and sewage treatment stations, as the methods currently in use are inefficient. Furthermore, OCTH was stable for up to 25 h in two buffered solutions with pH values of 2.10 and 5.45, as supporting electrolytes. The voltammetric behavior of the RuO_2 electrode in the buffered solutions at different pH values in the absence OTCH exhibited a cathodic shift as a function of the variation of pH for all redox transitions and a facilitation of the oxygen evolution reaction (OER).

Cyclic voltammetry studies of the RuO_2 electrode in the presence of OCTH showed that its electrooxidation occurs near the oxygen evolution reaction (OER) and demonstrated the formation of a resistive film that blocks the surface active sites of the electrode. The active sites were unblocked with an intense release of oxygen in the absence of the antibiotic by application of a constant anodic current of +100 mA. The release of O_2 facilitated the removal of the organic film by mechanic and oxidative ways. The chemical oxidation of the organic film by the O_2 species must not be disconsidered. The unblocking of the electrode surface was also observed during electrolysis, since it was done under conditions that simultaneously caused the oxygen evolution reaction (OER). The kinetics studies of the electrooxidation of OTCH using the RuO_2 electrode showed pseudo-first order kinetics in relation to OTCH concentration and a higher rate constant at 5.45.

The microbiological studies using a RuO_2 electrode (geometric area of 2 cm^2) showed that the electrochemical degradation of a 2.01×10^{-3} mol dm^{-3} OCTH in buffered solution at pH 5.45 occurs rapidly, such that antibacterial activity is lost after only 120 min of electrolysis and requires little energy consumption. It should be noted that the OTCH concentration investigated in electrodegradation was about 250-fold as large as its minimum inhibitory concentration (MIC) of 4.0 μg cm^{-3}.

Acknowledgements The authors acknowledge the financial support from Fundação de Amparo à Pesquisa do Estado de Minas Gerais, FAPEMIG (Process EDT 359/05), Universidade Federal dos Vales do Jequitinhonha e Mucuri / UFVJM, Brazil, and TiBrasil Titânio Ltda by donation of the Ti.

References

1. Kolpin DW, Skopec M, Meyer MT, Furlong ET, Zaugg SD (2004) Sci Total Environ 328:119
2. Jara CC, Fino D, Specchia V, Saracco G, Spinelli P (2007) Appl Catal B 70:479
3. Balcioğlu IA, Ötker M (2003) Chemosphere 50:85
4. Bower CK, Daeschel MA (1999) Int J Food Microbiol 50:33
5. Guardabassi L, Wong DMAL, Dalsgaard A (2002) Water Res 29:1955
6. Guillemot D (1999) Curr Opin Microbiol 2:494
7. Mulroy A (2001) Water Environ Technol 13:32
8. Rabolle M, Spliid NH (2000) Chemosphere 40:715
9. Tzoc E, Arias ML, Valiente C (2004) Rev Bioméd 15:165
10. Miranda CD, Castillo G (1998) Sci Total Environ 224:167
11. Stumpf M, Ternes TA, Wilken R, Rodrigues SV, Baumann W (1999) Sci Total Environ 225:135
12. Ternes TA, Stumpf M, Mueller J, Haberer K, Wilken RD, Servos M (1999) Sci Total Environ 225:81
13. Richardson ML, Brown JM (1985) Pharm Pharmacol 37:1
14. Küremer K, Al-Ahmad A, Mersch-Sundermann V (2000) Chemosphere 40:701
15. Halling SB, Nors NS, Lankzky PF, Ingerslev F, Holten LHC, Jorgensen SE (1998) Chemosphere 36:357
16. Takahashi N, Nakal T, Satoh Y, Katoh Y (1994) Water Res 28:1563
17. Scott JP, Ollis D (1995) Environ Prog 14:88
18. Alvares ABC, Diaper C, Parsons S (2001) Environ Technol 22:409
19. Beer B (1996) Neth Pat Appl 216 (1957): 199, US Pat 3,236,756
20. De Nora O, Nidloa A, Trisoglio G, Bianchi G (1973) Br Pat 1 339:576
21. Calza P, Medana C, Pazzi M, Baiocchi C, Pelizzetti E (2004) Appl Catal B 53:63
22. Turiel E, Bordin G, Rodriguez AR (2005) J Environ Monit 7:189
23. González O, Sans C, Esplugas S (2007) J Hazard Mater 146:459
24. Wang X, Hu JM, Hsing IM (2004) J Electroanal Chem 562:73
25. Shieh DT, Hwang BJ (1995) J Electrochem Soc 142:816
26. Garavaglia R, Mari CM, Trasatti S (1984) Surf Technol 23:41
27. Rossi A, Boodts JFC (2002) J Appl Electrochem 35:735

28. Schimitt MO, Schneider S (2000) Phys Chem Comm 3:42
29. McCormick J, Jensen E, Miller R, Doerschuk A (1960) J Am Chem Soc 82:3381
30. Yuen MF, Lauks I, Dautremont-Smith WC (1983) Solid State Ionics 11:19
31. Burke LD, Whelan DP (1981) J Electroanal Chem 124:333
32. Comninellis Ch, De Battisti A (1996) J Chim Phys 93:673
33. Fóti G, Gandini D, Comninellis Ch, Perret A, Haenni W (1999) Electrochem Solid-State Lett 2:228
34. Hu JM, Zhang JQ, Meng HM, Zhang JT, Cao CN (2005) Electrochim Acta 50:5370
35. Andrade AR, Donate PM, Alves PPD, Fidellis CHV (1998) J Electrochem Soc 145:3839
36. Doubova LM, De Battisti A, Daolio S, Pagura C, Barison S, Gerbasi R, Battiston G, Guerriero P, Trasatti S (2004) Russian J Electrochem 40:1115
37. Bard AJ, Faulkner RL (1980) Electrochemical methods: fundamental and applications. Wiley, New York
38. Santos MC, Cogo LC, Tanimoto ST, Calegaro ML, Bulhões LOS (2006) Appl Surf Science 253:1817
39. Malpass GRP, Miwa DW, Machado SAS, Olivi P, Motheo AJ (2006) J Hazard Mater 137:565
40. Mousty C, Foti G, Comninellis Ch, Reid V (1999) Electrochim Acta 45:451
41. Simond O, Schaller V, Comninellis Ch (1997) Electrochim Acta 42:2009
42. Foti G, Gandini D, Comninellis Ch, Perret A, Haenni W (1999) Electrochem Solid-State Lett 2:228
43. Fóti G, Gandini G, Comninellis Ch (1997) Curr Top Electrochem 5:71
44. Costa FIM, Lima PL, Machado SAS, Avaca LA (1998) Electrochim Acta 44:1515